INFECTION AND IMMUNITY, Aug. 2002, p. 4669–4677 Vol. 70, No. 8
0019-9567/02/$04.00+0 DOI: 10.1128/IAI.70.8.4669–4677.2002

Escherichia coli Shiga-Like Toxins Induce Apoptosis and Cleavage of Poly(ADP-Ribose) Polymerase via In Vitro Activation of Caspases

Joyce C. Y. Ching,[1,2] Nicola L. Jones,[1,3,4] Peter J. M. Ceponis,[1,5] Mohamed A. Karmali,[6] and Philip M. Sherman[1,2,3,5]*

Research Institute, Hospital for Sick Children,[1] Institute of Medical Science,[2] and Departments of Pediatrics,[3] Physiology,[4] and Laboratory Medicine & Pathobiology,[5] University of Toronto, Toronto, and Health Canada, Guelph,[6] Ontario, Canada

Received 15 January 2002/Returned for modification 28 February 2002/Accepted 23 April 2002

Shiga-like toxin-producing *Escherichia coli* causes hemorrhagic colitis and hemolytic-uremic syndrome in association with the production of Shiga-like toxins, which induce cell death via either necrosis or apoptosis. However, the abilities of different Shiga-like toxins to trigger apoptosis and the sequence of intracellular signaling events mediating the death of epithelial cells have not been completely defined. Fluorescent dye staining with acridine orange and ethidium bromide showed that Shiga-like toxin 1 (Stx1) induced apoptosis of HEp-2 cells in a dose- and time-dependent manner. Stx2 also induced apoptosis in a dose-dependent manner. Apoptosis induced by Stx1 (200 ng/ml) and apoptosis induced by Stx2 (200 ng/ml) were maximal following incubation with cells for 24 h (94.3% ± 1.8% and 81.7% ± 5.2% of the cells, respectively). Toxin-treated cells showed characteristic features of apoptosis, including membrane blebbing, DNA fragmentation, chromatin condensation, cell shrinkage, and the formation of apoptotic bodies, as assessed by transmission electron microscopy. Stx2c induced apoptosis weakly even at a high dose (1,000 ng/ml for 24 h; 26.7% ± 1.3% of the cells), whereas Stx2e did not induce apoptosis of HEp-2 cells. Thin-layer chromatography confirmed that HEp-2 cells express the Stx1-Stx2-Stx2c receptor, globotriaosylceramide (Gb3), but not the Stx2e receptor, globotetraosylceramide (Gb4). Western blot analysis of poly(ADP-ribose) polymerase (PARP), a DNA repair enzyme, demonstrated that incubation with Stx1 and Stx2 induced cleavage, whereas incubation with Stx2e did not result in cleavage of PARP. A pan-caspase inhibitor (Z-VAD-FMK) and a caspase-8-specific inhibitor (Z-IETD-FMK) eliminated, in a dose-dependent fashion, the cleavage of PARP induced by Shiga-like toxins. Caspase-8 activation was confirmed by detection of cleavage of this enzyme by immunoblotting. Cleavage of caspase-9 and the proapoptotic member of the Bcl-2 family BID was also induced by Stx1, as determined by immunoblot analyses. We conclude that different Shiga-like toxins induce different degrees of apoptosis that correlates with toxin binding to the glycolipid receptor Gb3 and that caspases play an integral role in the signal transduction cascade leading to toxin-mediated programmed cell death.

Shiga-like toxin-producing *Escherichia coli* (STEC), including the most common serotype, serotype O157:H7, is a bacterial enteropathogen capable of intimately binding to intestinal epithelium and producing Shiga-like toxins, which are associated with hemorrhagic colitis and the hemolytic-uremic syndrome in humans (2, 35). STEC can produce several distinct Shiga-like toxins in a strain-specific manner, including Shiga-like toxin 1 (Stx1), Stx2, and the Stx2 variants Stx2c (39), Stx2d1, Stx2d2 (23), Stx2e (28), Stx2f (38), and Stx2y (33).

Shiga-like toxins are multimeric toxins composed of an enzymatically active A subunit inserted into a pentamer of B subunits, which bind to the globotriaosylceramide (Gb3) glycolipid receptor present on the plasma membrane of certain eukaryotic cells (31, 43, 47). An exception is Stx2e, which binds primarily to globotetraosylceramide (Gb4) (9). Following receptor binding, the A subunit enters the host cell and inhibits protein synthesis by cleaving 28S rRNA, thereby causing cell death (13). Aside from the cytotoxic (late-effect) events, there is also an early response to Shiga-like toxins through an independent pathway, known as apoptosis or programmed cell death (37).

Apoptosis is a physiological event important in a diverse array of biological processes ranging from embryo development (52) to bacterial infection (53). Caspases play an integral role in the signal transduction pathway leading to apoptosis. Caspases are cysteine proteolytic enzymes that mediate apoptosis by cleaving aspartic acid residues in order to activate downstream effectors and substrates (6). A substrate for caspase-3 is poly(ADP-ribose) polymerase (PARP), a 116-kDa enzyme involved in DNA repair (51). Activated caspase-3 cleaves PARP between amino acids 216 and 217, generating 89- and 24-kDa inactive fragments. The loss of PARP function precludes DNA repair, which contributes to the apoptotic phenotype (34).

Apoptosis of intestinal epithelial cells decreases barrier function (1) and could provide a mechanism for Shiga-like toxins to enter the bloodstream (17). Previous work in our laboratory has shown that Stx1 induces apoptosis in HEp-2 cells through activation of caspase-3 and enhanced Bax expression (19). To further delineate the intracellular events mediating Shiga-like toxin-induced apoptosis of epithelial cells, in this study we tried to determine the effects of Shiga-like toxin variants on apoptosis and to define the roles of PARP cleav-

* Corresponding author. Mailing address: Rm. 8411, Hospital for Sick Children, 555 University Ave., Toronto, Ontario M5G 1X8, Canada. Phone: (416) 813-7734. Fax: (416) 813-6531. E-mail: sherman@sickkids.ca.

age, caspase activation, and BID activation in toxin-challenged host cells.

MATERIALS AND METHODS

Cell culture. The transformed human laryngeal epithelial cell line HEp-2 (CCL23; American Type Culture Collection, Manassas, Va.),which expresses Gb3 but not Gb4 (43), was cultured in minimum essential medium supplemented with 15% (vol/vol) heat-inactivated fetal bovine serum, 0.1% sodium bicarbonate, 1% amphotericin B (Fungizone), and 2% penicillin-streptomycin (Life Technologies GIBCO BRL, Grand Island, N.Y.). HEp-2 cells are widely employed as a model system for studying host epithelial cell responses to bacterial infections (8). HEp-2 cells were seeded onto 60-mm petri dishes ($\sim 3 \times 10^6$ cells) and grown to confluence at 37°C in the presence of 5% CO_2 prior to incubation with toxin.

Bacterial toxins. Stx1 was kindly provided by Clifford Lingwood (Hospital for Sick Children, Toronto, Ontario, Canada) (31). Stx2e was kindly provided by Carlton Gyles (University of Guelph, Guelph, Ontario, Canada) (46).

Caspase inhibitors. The pan-caspase inhibitor Z-VAD-FMK (Calbiochem, San Diego, Calif.) and the specific caspase-8 inhibitor Z-IETD-FMK (R&D Systems, Minneapolis, Minn.) were resuspended in dimethyl sulfoxide and preincubated with HEp-2 cells at various concentrations for 2 h prior to toxin treatment for 24 h. Dimethyl sulfoxide alone served as a vehicle control.

Expression of Gb3 and Gb4: thin-layer chromatography. Lipids were isolated from $\sim 3 \times 10^6$ HEp-2 cells as described previously (26). Briefly, cells were mixed in a chloroform-methanol solution (2:1, vol/vol) and shaken overnight at room temperature. Following addition of distilled water, the solution was allowed to separate overnight into polar and nonpolar layers. The nonpolar layer was extracted and evaporated by using nitrogen gas. The remaining residue solute was then resuspended in 50 μl of chloroform-methanol (2:1, vol/vol), and 30 μl of the lipid extract was loaded onto a plastic thin-layer chromatography plate. Lipids were resolved by polarity with a solvent mixture containing chloroform, methanol, and water (65:25:4, vol/vol/vol) and were stained with orcinol for visualization. Lipid standards for Gb3 and Gb4 from human kidney tissue served as controls.

Shiga-like toxin treatment of HEp-2 cells. Briefly, HEp-2 cells were incubated with toxin and then serum starved overnight as previously described (19) prior to treatment with Shiga-like toxins at various concentrations (1 to 1,000 ng/ml) and at various times (zero time to 32 h). Staurosporine (1 μM) was incubated with HEp-2 cells for 24 h as a positive control for the induction of apoptosis (4). As a positive control for necrosis, cells were subjected to freeze-thawing, a severe insult to cells that induced cell death (19).

Assessment of apoptosis. (i) Transmission electron microscopy. Cells were grown to confluence in 60-mm petri dishes, serum starved overnight, and incubated with Shiga-like toxins for 24 h, as described above. Suspended cells and trypsinized adherent cells were pooled and then pelleted by centrifugation. The cells were fixed with 2% glutaraldehyde in 0.1 M phosphate buffer, exposed to 2% osmium tetroxide, and then dehydrated by using graded acetone washes. Samples were embedded in epoxy resin, sectioned, and placed onto 300-mesh copper grids. The grids were stained with uranyl acetate and lead salts, and apoptotic cells were detected by transmission electron microscopy at an accelerating voltage of 65 kV (12).

(ii) Fluorescent dye staining. Acridine orange is a cell-permeable dye that intercalates DNA to appear green. Ethidium bromide enters cells with disrupted membrane integrity and intercalates RNA and double-stranded DNA to appear orange. Thus, differential uptake and binding of these dyes determine early and late stages of apoptosis and necrosis (15, 29).

Suspended cells were pooled with trypsinized adherent cells, pelleted, and then resuspended in 0.5 ml of 1% phosphate-buffered saline (PBS). Acridine orange-ethidium bromide in PBS (5 μl of a 100-μg/ml solution) was added to a 0.1-ml cell suspension, and stained cells were observed by fluorescence microscopy, as previously described (19). A total of 300 cells were counted in multiple randomly selected fields, and the percentage of apoptotic cells was then calculated.

Western blotting. (i) Whole-cell protein extraction. Confluent cells were serum starved and treated with toxin, as described above. Suspended cells were pooled with cells collected with a rubber policeman from 60-mm petri dishes in radioimmunoprecipitation assay buffer (1% Nonidet P-40, 0.5% sodium deoxycholate, and 0.1% sodium dodecyl sulfate [SDS] in PBS) supplemented with 150 mM NaCl, 25 μg of aprotinin per ml, 2 μg of leupeptin per ml, 2 μg of pepstatin per ml, 1 nM sodium *ortho*-vanadate, 50 mM sodium fluoride, and 100 μg of phenylmethylsulfonyl fluoride per ml. (Sigma, Oakville, Ontario, Canada). The cells were sheared by five passages through a 21-gauge needle, left on ice for 1 h, and then centrifuged at 12,000 rpm in a Sorvall SS-34 rotor for 10 min at 4°C. Aliquots of the supernatant were stored at −80°C until analysis.

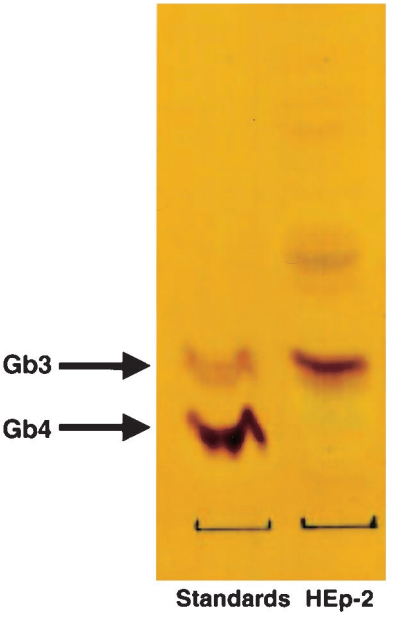

FIG. 1. Gb3, and not Gb4, is present in HEp-2 cells, as determined by thin-layer chromatography of extracted lipids from HEp-2 cells.

(ii) Immunoblot assay. Samples were dissolved in SDS sample buffer, boiled for 4 min, and subjected to electrophoresis through an 8% polyacrylamide gel (or a 15% polyacrylamide gel for BID, caspase-8, and caspase-9 immunoblots). After SDS-polyacrylamide gel electrophoresis, proteins were transferred onto nitrocellulose membranes (Pall Corporation, East Hills, N.Y.) for 1 h at 4°C. Residual binding sites on the membranes were then blocked with 5% (wt/vol) nonfat dry milk in Tris-buffered saline–0.05% Tween 20 (TBST) for 1 h at room temperature. Subsequently, each membrane was incubated with polyclonal rabbit anti-human PARP antibody (1:1,000 dilution), monoclonal mouse anti-human caspase-8 1C12 antibody (1:1,000 dilution), polyclonal rabbit anti-human caspase-9 antibody (1:1,000 dilution), or polyclonal rabbit anti-human BID antibody (1:1,000 dilution; Cell Signaling Technologies, Mississauga, Ontario, Canada) overnight at 4°C. The blots were rinsed twice in distilled water, washed three times in TBST (5 min each), and incubated with donkey anti-rabbit immunoglobulin G horseradish peroxidase-conjugated antibody (1:1,000 dilution; Santa Cruz Biotechnology, Santa Cruz, Calif.) or anti-mouse immunoglobulin G horseradish peroxidase-linked antibody (1:1,000 dilution; Cell Signaling Technologies) for 1 h at room temperature, and then they were developed by using a Western blotting chemiluminescence luminol reagent (Santa Cruz Biotechnology). To monitor protein loading levels in different samples, membranes were stripped and reprobed to determine expression of β-actin (1:1,000 dilution; Santa Cruz Biotechnology). Band densities were quantified with a chemiluminescence detector (Santa Cruz Biotechnology) and were analyzed with Fluorchem software (Alpha Innotech Corporation, San Leandro, Calif.) to compare levels of protein.

Statistical analysis. Results are expressed below as means ± standard errors. Analysis of variance (ANOVA) was used to compare both the percentages of apoptotic cells determined by fluorescent dye staining and the amounts of PARP cleavage determined by immunoblot densitometry.

RESULTS

HEp-2 cells express Gb3 but not Gb4. Thin-layer chromatograms displayed expression of the Stx1, Stx2, and Stx2c receptor, Gb3, in HEp-2 cell lipid extracts (Fig. 1). In contrast, Gb4, the Stx2e receptor, was not detectable in the HEp-2 cell plasma membranes.

Stx1 induces morphologically defined apoptosis in HEp-2

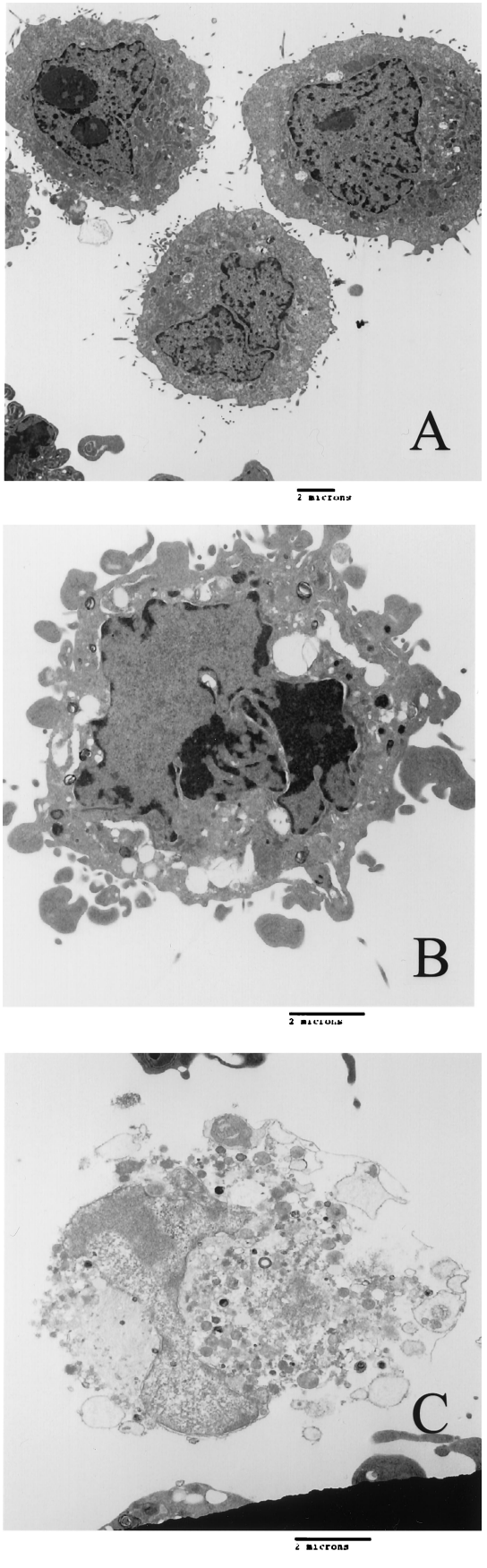

cells. Transmission electron microscopy was utilized to assess Stx1-induced apoptosis in HEp-2 cells, which express Gb3, a Shiga-like toxin (Stx1, Stx2, and Stx2c) receptor. Compared to untreated cells (Fig. 2A), apoptotic cells displayed the characteristic morphology of chromatin condensation and margination, fragmentation of nuclei, cell blebbing, and cell shrinkage (Fig. 2B). These cells were distinguishable from necrotic cells, which were characterized by a loss of membrane integrity and selective permeability, which resulted in swelling of the cells and leakage of the cytoplasmic contents (Fig. 2C).

Apoptosis was also assessed by the complementary, semiquantitative fluorescent dye technique by using acridine orange and ethidium bromide. Nuclear chromatin condensation was observed in cells treated with Stx1, as assessed by fluorescence microscopy (Fig. 3A and B). Necrotic HEp-2 cells were distinguished by uptake of ethidium bromide and maintenance of nuclear morphology (Fig. 3C). There was only a low level of necrosis induced by Shiga-like toxin treatment (1 to 5%) that was quantified by fluorescent dye staining. Stx1 at a concentration of 10 ng/ml induced apoptosis of HEp-2 cells in a time-dependent manner (Fig. 4A), and maximal induction of apoptosis occurred after 24 h of incubation (38.9% ± 3.8%; $P < 0.005$, as determined by ANOVA). HEp-2 cells incubated with Stx1 at various concentrations for 24 h exhibited a dose-dependent increase in apoptosis (Fig. 4B), and maximal induction of apoptosis occurred at a concentration of 200 ng/ml (94.3% ± 1.8%; $P < 0.001$, as determined by ANOVA).

Stx2 induces apoptosis in HEp-2 cells. Stx2 also induced apoptosis of HEp-2 cells, as confirmed by transmission electron microscopy (Fig. 5A) and fluorescence microscopy. HEp-2 cells incubated with various concentrations of Stx2 for 24 h showed a dose-dependent increase in apoptosis (Fig. 5B). The maximum amount of apoptosis detected occurred at an Stx2 concentration of 200 ng/ml (81.7% ± 5.2%; $P < 0.001$, as determined by ANOVA).

Effect of Stx2 variants on HEp-2 cell apoptosis. As assessed by fluorescence microscopy (Fig. 5C), Stx2c induced apoptosis of HEp-2 cells only when it was employed at a high dose (1,000 ng/ml; 26.7% ± 1.3%; $P < 0.001$, as determined by ANOVA). Stx2e, which is known to bind to Gb4 (46), did not induce apoptosis of HEp-2 cells even at a concentration of 1,000 ng/ml (Fig. 5C).

Stx1 and Stx2 induce cleavage of PARP. As shown in Fig. 6A, whole-cell protein extracts taken from HEp-2 cells incubated with Stx1 (10 ng/ml) for 0 to 32 h showed that there was a time-dependent increase in the amount of PARP cleaved. Incubation with Stx1 at concentrations of 0 to 100 ng/ml showed that there was a dose-dependent increase in the cleav-

FIG. 2. Stx1 induces apoptosis of HEp-2 cells, as assessed by transmission electron microscopy. (A) HEp-2 cells grown in medium alone, displaying normal morphology. (B) HEp-2 cells treated with Stx1 (100 ng/ml) for 24 h, displaying membrane blebbing, chromatin condensation, DNA fragmentation, and the formation of apoptotic bodies, consistent with apoptosis. (C) Necrotic HEp-2 cell after Shiga-like toxin treatment, showing loss of membrane integrity, cell swelling, and leakage of cytoplasmic contents. The micrographs are electron micrographs that are representative of at least three separate experiments. Bars = 2 μm.

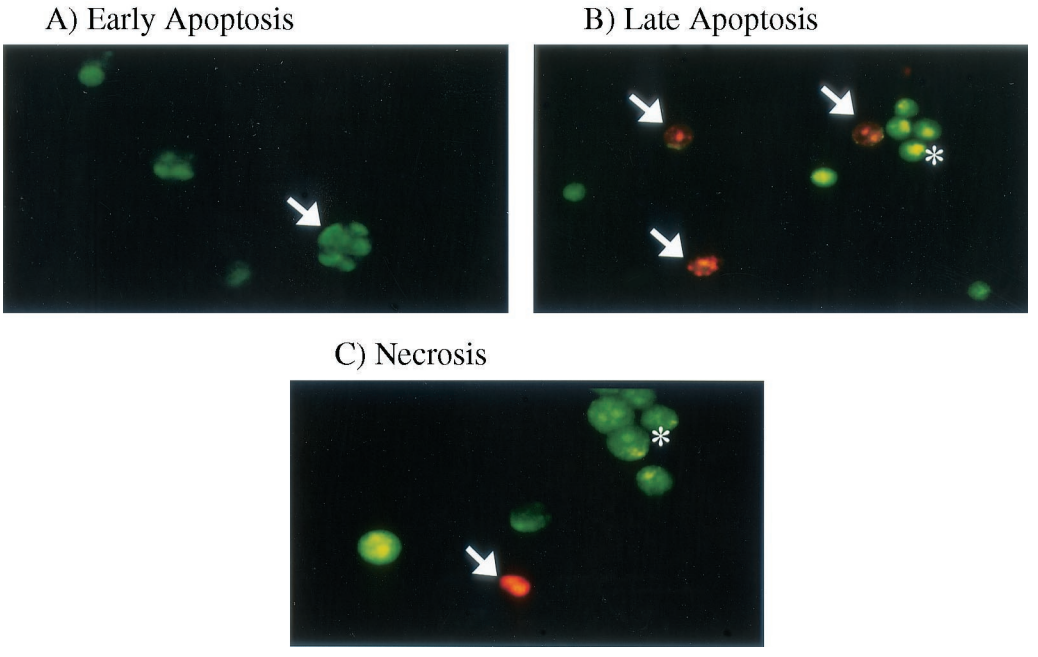

FIG. 3. Stx1-induced apoptosis, as assessed by acridine orange and ethidium bromide fluorescent dye staining. (A) Early apoptotic HEp-2 cell (arrow), showing the presence of green patches of fragmented and condensed chromatin. (B) Late apoptotic cells fluoresce orange (arrows), whereas viable cells are uniformly green (asterisk). As the plasma membrane loses its integrity, ethidium bromide enters the cell and intercalates fragmented DNA, staining the cell red. (C) Necrotic cell (arrow) that has lost its selective permeability, allowing ethidium bromide to intercalate DNA and produce a uniform red color. Viable cells are uniformly green (asterisk). Original approximate magnifications, ×400.

age of PARP (Fig. 6B). For example, incubation with Stx1 at a concentration of 100 ng/ml resulted in a (5.4 ± 1.3)-fold increase in PARP cleavage compared with the cleavage in the medium control.

Incubation with Stx2 at concentrations ranging from 0 to 100 ng/ml also resulted in dose-dependent cleavage of PARP (Fig. 7A). As determined by densitometry, incubation with 100 ng of Stx2 per ml resulted in a (3.7 ± 0.8)-fold increase in PARP cleavage compared with the cleavage in the medium control.

Stx2c, but not Stx2e, mediates PARP cleavage. As shown in Fig. 7B, incubation of HEp-2 cells for 24 h with Stx2c (100 and 1,000 ng/ml) induced cleavage of PARP. Incubation with Stx2c at a concentration of 100 ng/ml resulted in a (2.6 ± 0.6)-fold increase in PARP cleavage compared to the cleavage in the medium control. Incubation with Stx2c at a higher concentration (1,000 ng/ml) resulted in a (4.6 ± 1.7)-fold increase in PARP cleavage. In contrast, even at a dose of 1,000 ng/ml Stx2e did not induce detectable cleavage of PARP in HEp-2 cells.

Caspase inhibitors eliminate Stx1- and Stx2-induced PARP cleavage. Increasing concentrations of the pan-caspase inhibitor Z-VAD-FMK, which targets caspase-1, caspase-3, caspase-4, and caspase-7 (42), eliminated PARP cleavage induced by Stx1 (10 ng/ml) (Fig. 8A and B) ($P < 0.01$, as determined by ANOVA), Stx2, and Stx2c (data not shown) in a dose-dependent manner. A specific caspase-8 inhibitor, Z-IETD-FMK, also decreased the amount of PARP cleavage induced by Stx1 (Fig. 8C).

Stx1 induces cleavage of caspase-8 and caspase-9. Incubation of HEp-2 cells for 6 h with Stx1 (10 and 100 ng/ml) induced cleavage of caspase-8 (Fig. 9A) and caspase-9 (Fig.

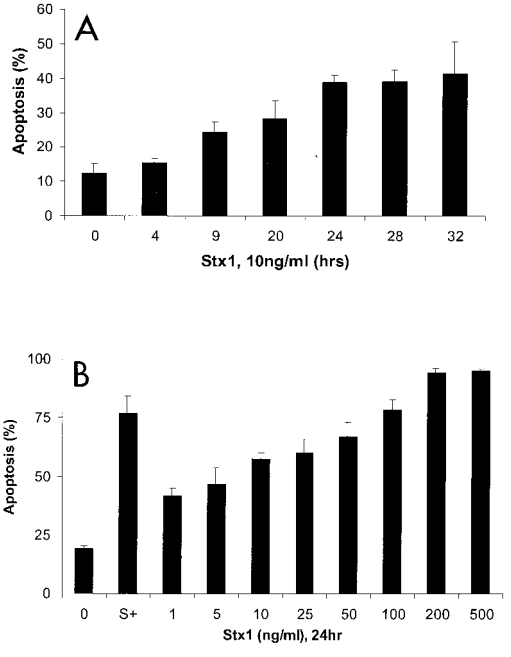

FIG. 4. Stx1 induces apoptosis in HEp-2 cells in a time- and dose-dependent manner. (A) Apoptosis was quantified by fluorescent dye staining of HEp-2 cells treated with Stx1 (10 ng/ml) for various times ($n = 3$ for each time point; $P < 0.005$, as determined by ANOVA). (B) HEp-2 cells treated with various concentrations of Stx1 for 24 h. Apoptosis was quantified by fluorescent dye staining. Staurosporine (1 μM) (bar S+), a known inducer of apoptosis (4), was used as a positive control. Untreated cells (bar 0) served as the negative control ($n \geq 6$; $P < 0.001$, as determined by ANOVA).

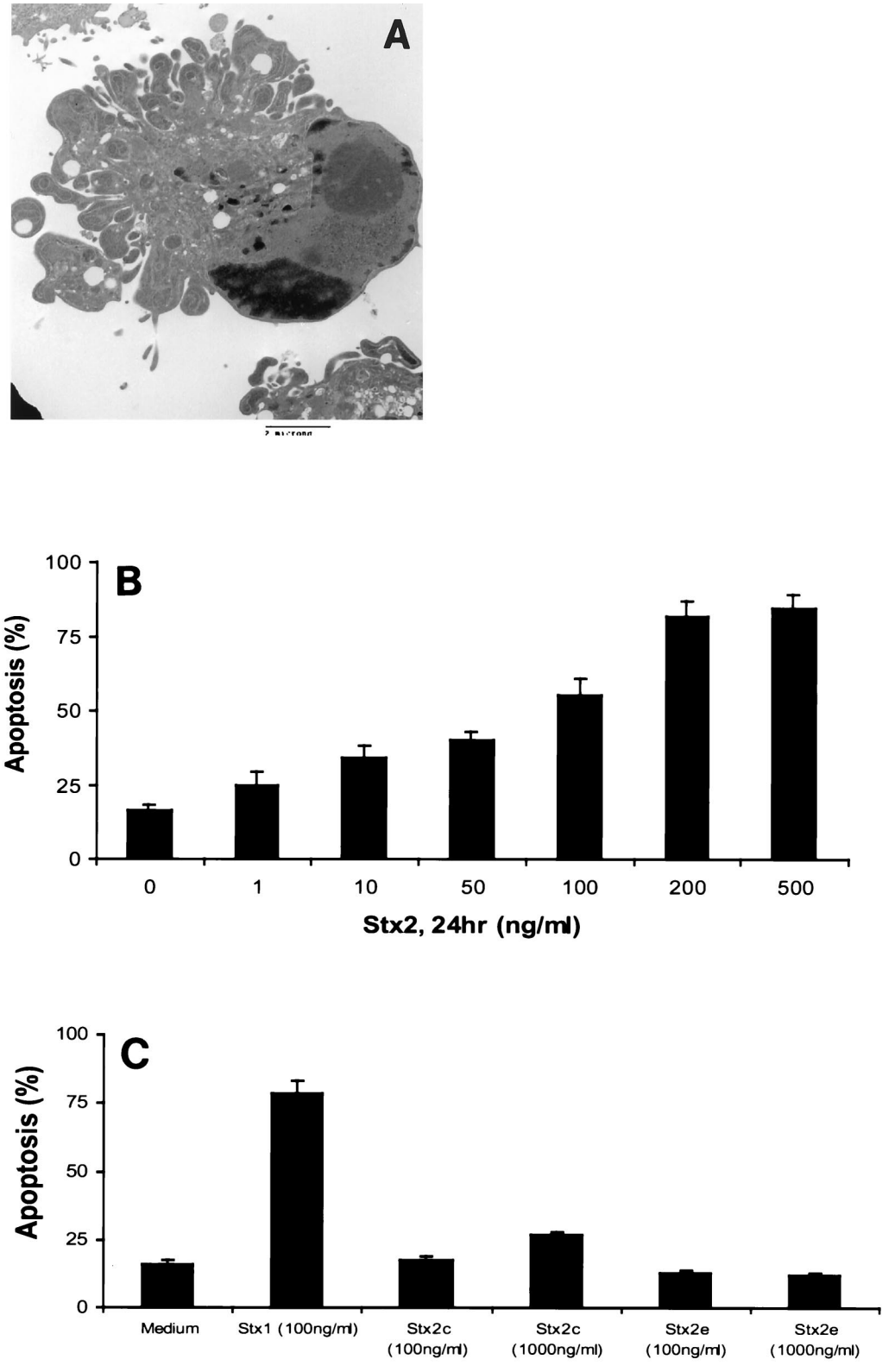

FIG. 5. Induction of apoptosis by Stx2 and Stx2c in HEp-2 cells. (A) Transmission electron micrograph showing a HEp-2 cell treated with Stx2 (100 ng/ml) for 24 h undergoing apoptosis, as shown by the characteristic morphological features of apoptosis. Bar = 2 μm. (B) Fluorescence microscopy showed that incubation with Stx2 for 24 h induced apoptosis in a dose-dependent manner ($n \geq 6$; $P < 0.001$, as determined by ANOVA). (C) The Stx2 variant Stx2c (1,000 ng/ml) ($n = 5$; $P < 0.001$, as determined by ANOVA), but not Stx2e, induced apoptosis of HEp-2 cells.

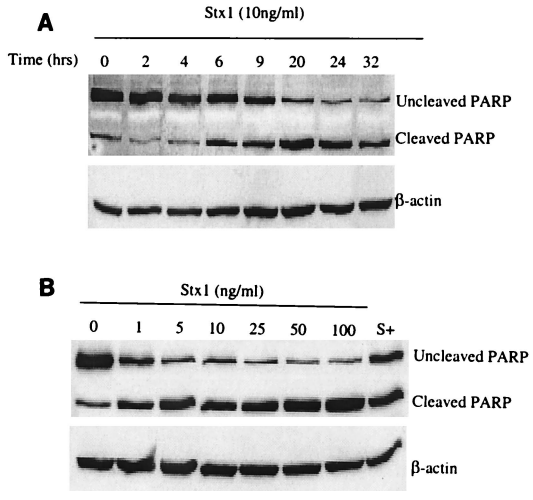

FIG. 6. Stx1 induces PARP cleavage in a time- and dose-dependent manner, as determined by Western blot analysis of HEp-2 whole-cell protein lysates probed with PARP antibody. (A) Immunoblot of HEp-2 lysates following incubation with Stx1 (10 ng/ml), demonstrating PARP cleavage in a time-dependent fashion. Membranes were probed for β-actin to determine protein loading in each lane. (B) Immunoblot showing Stx1 (10 ng/ml)-induced PARP cleavage in HEp-2 cells in a dose-dependent manner. Staurosporine (1,000 nM) (lane S+) was used as a positive control. Membranes were probed for β-actin to determine protein loading in each lane.

9B). Incubation for 2 h with Stx1 (100 ng/ml) did not induce cleavage of caspase-8, whereas incubation for 8 h induced cleavage of caspase-8 compared to the cleavage in the medium control, demonstrating that there was a time-dependent response.

Stx1 induces cleavage of BID. As shown in Fig. 10, whole-cell protein extracts of HEp-2 cells incubated with Stx1 (10 ng/ml) for 0 to 24 h showed that there was an increase in the amount of truncated BID compared to the amount in the medium control.

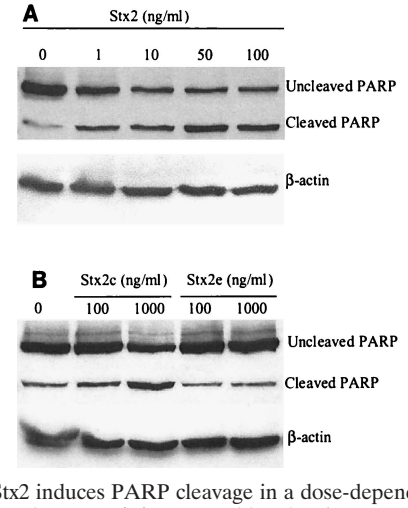

FIG. 7. Stx2 induces PARP cleavage in a dose-dependent manner, whereas Stx2e does not. (A) Immunoblot showing PARP cleavage in HEp-2 cells following 24 h of treatment with various concentrations of Stx2. Membranes were probed for β-actin to determine protein loading in each lane. (B) Stx2c (1,000 ng/ml) induces PARP cleavage, whereas Stx2e does not induce cleavage of PARP. Membranes were probed for β-actin to determine protein loading in each lane.

DISCUSSION

In this study, by employing a series of complementary techniques, we showed that Stx1, Stx2, and Stx2c each induce apoptosis of human epithelial cells that express Gb3. Apoptosis is a physiological event important in a variety of microbial infections (50). Indeed, it could provide an explanation for how Shiga-like toxins breach the epithelial barrier in the intestine. STEC is ingested orally through inadvertent consumption of contaminated food or water, colonizes the gut epithelium, and, among other pathogenic strategies, secretes toxins into the lumen of the intestine (10). Current evidence favors toxin-mediated vascular endothelial cell damage as the basis for hemorrhagic colitis and hemolytic-uremic syndrome. Thus, toxins crossing the mucosal intestinal epithelial barrier are likely to be a critical initial step in the pathogenesis of disease (32). An increase in apoptosis of gut epithelial cells could result in disruption of intestinal barrier function that allows Shiga-like toxins to pass more easily into the vascular system. Stx1 and Stx2 also induce apoptosis in other epithelial cells (20, 21, 40, 44) and injure other cell types, including astrocytoma cells (3) and Burkitt's lymphoma cells (22).

Although Stx1, Stx2, and Stx2c are known to bind to the Gb3 receptor (25, 30), differences in the amino acid sequences of the toxins influence binding affinities and potentially affect intracellular signaling events following toxin binding (36). This likely explains the various effects of the different Shiga-like toxins in inducing apoptosis of HEp-2 cells. Stx2e is known to bind primarily to Gb4, which is not present in HEp-2 cells (43), and this provides an explanation for the absence of apoptosis following exposure to Stx2e.

Intestinal epithelial cells from mice, humans, and certain immortalized gut epithelial cell lines (human colonic T84 cells) do not express Gb3 and are resistant to the cytotoxic effects of Shiga-like toxins (41). However, proinflammatory cytokine release, such as release of interleukin-1 and tumor necrosis factor alpha, can induce the expression of Gb3 on the surfaces of human glomerular epithelial cells (16). Moreover, Gb3 expression in the human colonic CaCo-2 cell line is enhanced following incubation with butyric acid, which confers toxin sensitivity on previously resistant cells (18, 45). Thus, inflammatory cytokines released during infection in vivo could result in epithelial Gb3 expression.

Here, we show that PARP cleavage is caused by Shiga-like toxin treatment of human epithelial cells. PARP is cleaved as a substrate of activated caspases, including caspase-3, and, accordingly, serves as an indicator of apoptosis (11). Furthermore, Stx1 has previously been shown to activate caspase-3 (19). In this study, immunoblot analysis of PARP cleavage proved to be a sensitive assay for detecting apoptosis.

This is the first study to find that activation of both caspase-8 and caspase-9 is involved in Shiga-like toxin-induced signal transduction that causes apoptosis of epithelial cells. We provide pharmacological evidence that caspase-8 activity contributes to eliciting PARP cleavage. Furthermore, we showed that there is cleavage of caspase-8 (57 to 55 kDa) and caspase-9 (47 kDa) by immunoblotting for cleaved fragments (43 to 41 and

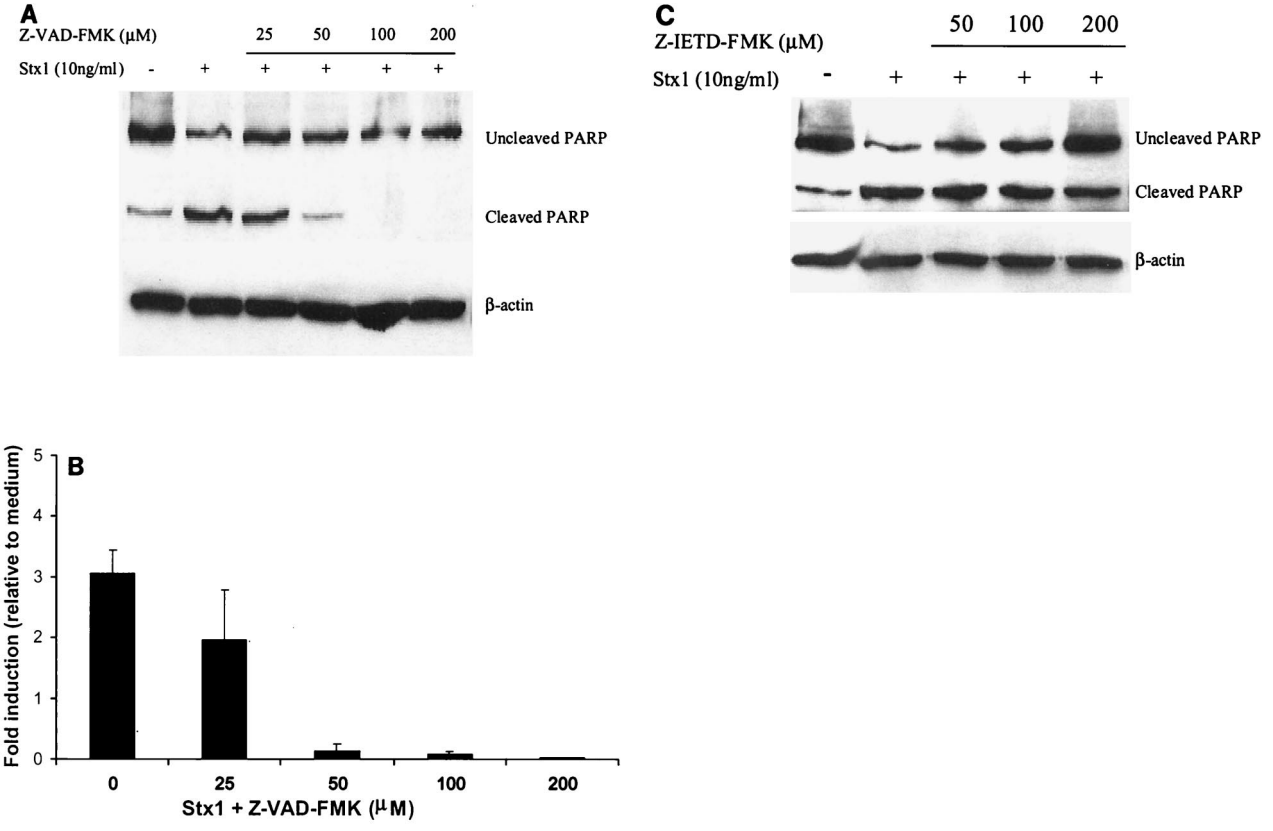

FIG. 8. Pan-caspase and specific caspase-8 inhibitors eliminate Stx1-induced PARP cleavage. (A) Pretreatment of HEp-2 cells with the pan-caspase inhibitor Z-VAD-FMK for 2 h at 37°C prior to Stx1 (10 ng/ml) treatment for 24 h eliminated PARP cleavage induced by the toxin. Membranes were probed for β-actin to determine protein loading in each lane. (B) Densitometry of Western blot of Stx1-mediated PARP cleavage inhibited by Z-VAD-FMK. The results of three individual experiments are shown ($P < 0.01$, as determined by ANOVA). (C) Pretreatment of HEp-2 cells with the caspase-8 inhibitor Z-IETD-FMK 2 h prior to toxin treatment for 24 h resulted in decreased PARP cleavage induced by Stx1.

37 to 35 kDa, respectively). Caspases play an integral role in mediating the intracellular signaling events that result in apoptosis (7). Thus, caspase-8 is involved in Shiga-like toxin-mediated apoptosis of epithelial cells; however, whether Shiga-like toxin activates caspase-8 directly via Gb3 binding or indirectly through death receptors and ligands remains to be elucidated. Activation of caspase-8 likely results in cleavage of BID, which then induces cytochrome *c* release from the mitochondria (24, 27) and thereby activates procaspase-3. In support of this contention, we observed increased expression of truncated BID in response to Stx1.

BID is localized in the cytosol of cells as an inactive precursor and acts as the link between activated caspase-8 and the mitochondrion death pathway (24, 27). Proteolytic cleavage by active caspase-8 cleaves 22-kDa full-length BID into 15-kDa active truncated BID (48). This carboxyl active fragment of BID triggers the homo-oligomerization of proapoptotic BAK and BAX proteins, which results in the release of cytochrome *c* from the mitochondria (14, 49). Indeed, BID activation provides a mechanistic explanation for the increase in Bax expression observed previously (19). These experiments define the Shiga-like toxin-mediated pathway through the activation of caspase-8, leading to the truncation of BID, thereby affecting the Bcl-2 proteins and the mitochondrial pore and downstream activation of caspase-9, resulting in apoptosis.

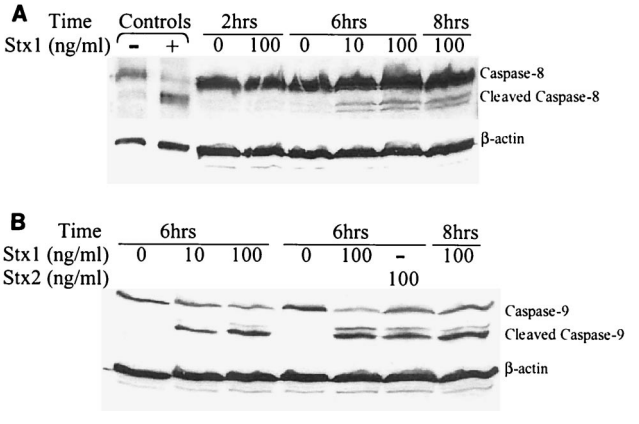

FIG. 9. Caspase-8 and caspase-9 are activated by Stx1. (A) Western blot analysis of HEp-2 whole-cell protein lysates probed with caspase-8 antibody. Lanes − and + contained control HeLa cells that were not treated and treated with cycloheximide-tumor necrosis factor (Cell Signaling Technologies), respectively. Incubation of HEp-2 cells with Stx1 (100 ng/ml) for 2 h did not induce cleavage of caspase-8. However, treatment of HEp-2 cells with Stx1 (10 and 100 ng/ml) for 6 and 8 h resulted in cleavage of caspase-8, demonstrating that caspase-8 cleavage occurred in a time-dependent fashion. Membranes were probed for β-actin to determine protein loading in each lane. (B) Whole-cell protein lysates probed with caspase-9 antibody. Treatment of HEp-2 cells with Stx1 (10 and 100 ng/ml) or Stx2 (100 ng/ml) for 6 h induced cleavage of caspase-9. Membranes were probed for β-actin to determine protein loading in each lane.

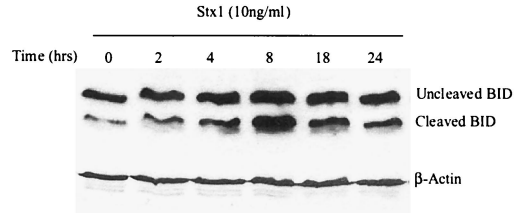

FIG. 10. Immunoblot demonstrating that Stx1 induces cleavage of BID in HEp-2 cells. Membranes were stripped and reprobed for β-actin to assess protein loading in each lane.

Insight into the molecular pathogenesis of STEC infection provides a basis for the development of novel treatment strategies to interrupt the disease process. Caspases are potential therapeutic targets for modulating apoptosis and provide a promising approach. For instance, treatment with a caspase inhibitor prevented cell death and reduced neurologic damage in an animal model of bacterial meningitis (5). Future studies aimed at preventing Shiga-like toxin-induced apoptosis in relevant animal models should help to develop novel therapeutics for use in the prevention and treatment of STEC-induced disease in humans.

ACKNOWLEDGMENTS

This research was supported by a Canadian Institutes of Health Research Studentship to J.C.Y.C. and by operating grants from the Canadian Institutes of Health Research. N.L.J. is the recipient of a Research Scholar Award from the American Digestive Health Foundation. P.M.S. is the recipient of a Canada Research Chair in Gastrointestinal Disease.

We thank Julia Hwang and Yew Ming Heng for technical support with electron microscopy and Mariola Mascarenhas for helping to prepare the toxins.

REFERENCES

1. **Abreu, M. T., A. A. Palladino, E. T. Arnold, R. S. Kwon, and J. A. McRoberts.** 2000. Modulation of barrier function during Fas-mediated apoptosis in human intestinal epithelial cells. Gastroenterology **119:**1524–1536.
2. **Agbodaze, D.** 1999. Verocytotoxins (Shiga-like toxins) produced by *Escherichia coli*: a minireview of their classification, clinical presentations and management of a heterogeneous family of cytotoxins. Comp. Immunol. Microbiol. Infect. Dis. **22:**221–230.
3. **Arab, S., M. Murakami, P. Dirks, B. Boyd, S. L. Hubbard, C. A. Lingwood, and J. T. Rutka.** 1998. Verotoxins inhibit the growth of and induce apoptosis in human astrocytoma cells. J. Neurooncol. **40:**137–150.
4. **Belmokhtar, C. A., J. Hillion, and E. Segal-Bendirdjian.** 2001. Staurosporine induces apoptosis through both caspase-dependent and caspase-independent mechanisms. Oncogene **20:**3354–3362.
5. **Braun, J. S., R. Novak, K. H. Herzog, S. M. Bodner, J. L. Cleveland, and E. I. Tuomanen.** 1999. Neuroprotection by a caspase inhibitor in acute bacterial meningitis. Nat. Med. **5:**298–302.
6. **Budihardjo, I., H. Oliver, M. Lutter, X., Luo, and X. Wang.** 1999. Biochemical pathways of caspase activation during apoptosis. Annu. Rev. Cell Dev. Biol. **15:**269–290.
7. **Cohen, G. M.** 1997. Caspases: the executioners of apoptosis. Biochem. J. **326:**1–16.
8. **Cossart, P., P. Boquet, S. Normark, and R. Rappuoli.** 2000. Cellular microbiology. ASM Press, Washington, D.C.
9. **DeGrandis, S., H. Law, J. Brunton, C. Gyles, and C. A. Lingwood.** 1989. Globotetraosylceramide is recognized by the pig edema disease toxin. J. Biol. Chem. **264:**12520–12525.
10. **Donnenberg, M. S., and T. S. Whittam.** 2001. Pathogenesis and evolution of virulence in enteropathogenic and enterohemorrhagic *Escherichia coli*. J. Clin. Investig. **107:**539–548.
11. **Duriez, P. J., and G. M. Shah.** 1997. Cleavage of poly(ADP-ribose) polymerase: a sensitive parameter to study cell death. Biochem. Cell Biol. **75:** 337–349.
12. **Dytoc, M. T., A. Ismaili, D. J. Philpott, R. Soni, J. L. Brunton, and P. M. Sherman.** 1994. Distinct binding properties of *eaeA*-negative verocytotoxin-producing *Escherichia coli* of serotype O113:H21. Infect. Immun. **62:**3494–3505.
13. **Endo, Y., K. Tsurugi, T. Yutsudo, Y. Takeda, T. Ogasawara, and K. Igarashi.** 1988. Site of action of verotoxin (VT2) from *Escherichia coli* O157:H7 and of Shiga toxin on eukaryotic ribosomes. RNA N-glycosidase activity of the toxins. Eur. J. Biochem. **171:**45–50.
14. **Eskes, R., S. Desagher, B. Antonsson, and J. C. Martinou.** 2000. Bid induces the oligomerization and insertion of Bax into the outer mitochondrial membrane. Mol. Cell. Biol. **20:**929–935.
15. **Grossman, J., S. Mohr, E. G. Lapentina, C. Fiocchi, and A. D. Levine.** 1998. Sequential and rapid activation of select caspases during apoptosis of normal intestinal epithelial cells. Am. J. Physiol. **274:**G1117–G1124.
16. **Hughes, A. K., P. K. Stricklett, D. Schmid, and D. E. Kohan.** 2000. Cytotoxic effect of Shiga toxin-1 on human glomerular epithelial cells. Kidney Int. **57:**2350–2359.
17. **Hurley, B. P., C. M. Thorpe, and D. W. Acheson.** 2001. Shiga toxin translocation across intestinal epithelial cells is enhanced by neutrophil transmigration. Infect. Immun. **69:**6148–6155.
18. **Jacewicz, M. S., M. Mobassaleh, S. K. Gross, K. A. Balasubramanian, P. F. Daniel, S. Raghavan, R. H. McCluer, and G. T. Keusch.** 1994. Pathogenesis of Shigella diarrhea: XVII. A mammalian cell membrane glycolipid, Gb3, is required but not sufficient to confer sensitivity to Shiga toxin. J. Infect. Dis. **169:**538–546.
19. **Jones, N. L., A. Islur, R. Haq, M. Mascarenhas, M. A. Karmali, M. H. Perdue, B. W. Zanke, and P. M. Sherman.** 2000. *Escherichia coli* Shiga toxins induce apoptosis in epithelial cells that is regulated by the Bcl-2 family. Am. J. Physiol. Gastrointest. Liver Physiol. **278:**G811–G819.
20. **Kaneko, K., N. Kiyokawa, Y. Ohtomo, R. Nagaoka, Y. Yamashiro, T. Taguchi, T. Mori, J. Fujimoto, and T. Takeda.** 2001. Apoptosis of renal tubular cells in Shiga-toxin-mediated hemolytic uremic syndrome. Nephron **87:**182–185.
21. **Kiyokawa, N., T. Taguchi, T. Mori, H. Uchida, N. Sato, T. Takeda, and J. Fujimoto.** 1998. Induction of apoptosis in normal human renal tubular epithelial cells by *Escherichia coli* Shiga toxins 1 and 2. J. Infect. Dis. **178:**178–184.
22. **Kiyokawa, N., T. Mori, T. Taguchi, M. Saito, K. Mimori, T. Suzuki, T. Sekino, N. Sato, H. Nakajima, Y. U. Katagiri, T. Takeda, and J. Fujimoto.** 2001. Activation of the caspase cascade during Stx1-induced apoptosis in Burkitt's lymphoma cells. J. Cell. Biochem. **81:**128–142.
23. **Kokai-Kun, J. F., A. R. Melton-Celsa, and A. D. O'Brien.** 2000. Elastase in intestinal mucus enhances the cytotoxicity of Shiga toxin type 2d. J. Biol. Chem. **275:**3713–3721.
24. **Li, H., H. Zhu, C. J. Xu, and J. Yuan.** 1998. Cleavage of BID by caspase 8 mediates the mitochondrial damage in the Fas pathway of apoptosis. Cell **94:**491–501.
25. **Lingwood, C. A.** 1999. Glycolipid receptors for verotoxin and *Helicobacter pylori*: role in pathology. Biochim. Biophys. Acta **1455:**375–386.
26. **Lingwood, C. A., B. Boyd, and A. Nutikka.** 2000. Analysis of interactions between glycosphingolipids and microbial toxins. Methods Enzymol. **312:** 459–473.
27. **Luo, X., I. Budihardjo, H. Zou, C. Slaughter, and X. Wang.** 1998. Bid, a Bcl2 interacting protein, mediates cytochrome c release from mitochondria in response to activation of cell surface death receptors. Cell **94:**481–490.
28. **MacLeod, D. L., C. L. Gyles, and B. P. Wilcock.** 1991. Reproduction of edema disease of swine with purified Shiga-like toxin-II variant. Vet. Pathol. **28:**66–73.
29. **McGahon, A. J., S. J. Martin, R. P. Bissonnette, A. Mahboubi, Y. Shi, R. J. Mogil, W. K. Nishioka, and D. R. Green.** 1995. The end of the (cell) line: methods for the study of apoptosis *in vitro*. Methods Cell Biol. **46:**153–185.
30. **Meyers, K. E., and B. S. Kaplan.** 2000. Many cell types are Shiga toxin targets. Kidney Int. **57:**2650–2651.
31. **Nyholm, P. G., J. L. Brunton, and C. A. Lingwood.** 1995. Modelling of the interaction of verotoxin-1 (VT1) with its glycolipid receptor, globotriaosylceramide (Gb3). Int. J. Biol. Macromol. **17:**199–204.
32. **O'Loughlin, E. V., and R. M. Robins-Browne.** 2001. Effect of Shiga toxin and Shiga-like toxins on eukaryotic cells. Microbes Infect. **3:**493–507.
33. **Parreira, V. R., and T. Yano.** 1998. Cytotoxin produced by *Escherichia coli* isolated from chickens with swollen head syndrome (SHS). Vet. Microbiol. **62:**111–119.
34. **Pieper, A. A., A. Verma, J. Zhang, and S. H. Snyder.** 1999. Poly (ADP-ribose) polymerase, nitric oxide and cell death. Trends Pharmacol. Sci. **20:**171–181.
35. **Proulx, F., E. G. Seidman, and D. Karpman.** 2001. Pathogenesis of Shiga toxin-associated hemolytic uremic syndrome. Pediatr. Res. **50:**163–171.
36. **Samuel, J. E., L. P. Perera, S. Ward, A. D. O'Brien, V. Ginsburg, and H. C. Krivan.** 1990. Comparison of the glycolipid receptor specificities of Shiga-like toxin type II and Shiga-like toxin type II variants. Infect. Immun. **58:** 611–618.
37. **Sandvig, K.** 2001. Shiga toxins. Toxicon **39:**1629–1635.
38. **Schmidt, H., J. Scheef, S. Morabito, A. Caprioli, L. H. Wieler, and H. Karch.** 2000. A new Shiga toxin 2 variant (Stx2f) from *Escherichia coli* isolated from pigeons. Appl. Environ. Microbiol. **66:**1205–1208.

39. **Schmitt, C. K., M. L. McKee, and A. D. O'Brien.** 1991. Two copies of Shiga-like toxin II-related genes common in enterohemorrhagic *Escherichia coli* strains are responsible for the antigenic heterogeneity of the O157:H− strain E32511. Infect. Immun. **59:**1065–1073.
40. **Taguchi, T., H. Uchida, N. Kiyokawa, T. Mori, N. Sato, H. Horie, T. Takeda, and J. Fujimoto.** 1998. Verotoxins induce apoptosis in human renal tubular epithelium derived cells. Kidney Int. **53:**1681–1688.
41. **Tesh, V. L., J. A. Burris, J. W. Owens, V. M. Gordon, E. A. Wadolkowski, A. D. O'Brien, and J. E. Samuel.** 1993. Comparison of the relative toxicities of Shiga-like toxins type I and type II for mice. Infect. Immun. **61:**3392–3402.
42. **Thornberry, N. A., and Y. Lazebnik.** 1998. Caspases: enemies within. Science **281:**1312–1316.
43. **Tyrrell, G. J., K. Ramotar, B. Toye, B. Boyd, C. A. Lingwood, and J. L. Brunton.** 1992. Alteration of the carbohydrate binding specificity of verotoxins from Galα1–4Gal to GalNAcβ1–3Galα1–4Gal and vice versa by site-directed mutagenesis of the binding subunit. Proc. Natl. Acad. Sci. USA **89:**524–528.
44. **Uchida, H., N. Kiyokawa, T. Taguchi, H. Horie, J. Fujimoto, and T. Takeda.** 1999. Shiga toxins induce apoptosis in pulmonary epithelium-derived cells. J. Infect. Dis. **180:**1902–1911.
45. **Van Setten, P. A., V. W. Van Hinsbergh, T. J. Van Der Velden, N. C. Van De Kar, M. Vermeer, J. D. Mahan, K. J. Assmann, L. P. Van Den Heuvel, and L. A. Monnens.** 1997. Effects of TNF alpha on verocytotoxin cytotoxicity in purified human glomerular microvascular endothelial cells. Kidney Int. **51:** 1245–1256.
46. **Waddell, T. E., B. L. Coomber, and C. L. Gyles.** 1998. Localization of potential binding sites for the edema disease verotoxin (VT2e) in pigs. Can. J. Vet. Res. **62:**81–86.
47. **Waddell, T. E., S. Head, M. Petric, A. Cohen, and C. Lingwood.** 1988. Globotriosyl ceramide is specifically recognized by the *Escherichia coli* verocytotoxin 2. Biochem. Biophys. Res. Commun. **152:**674–679.
48. **Wang, K., X. M. Yin, D. T. Chao, C. L. Milliman, and S. J. Korsmeyer.** 1996. BID: a novel BH3 domain-only death agonist. Genes Dev. **10:**2859–2869.
49. **Wei, M. C., T. Lindsten, V. K. Mootha, S. Weiler, A. Gross, M. Ashiya, C. B. Thompson, and S. J. Korsmeyer.** 2000. tBID, a membrane-targeted death ligand, oligomerizes BAK to release cytochrome c. Genes Dev. **14:**2060–2071.
50. **Weinrauch, Y., and A. Zychlinsky.** 1999. The induction of apoptosis by bacterial pathogens. Annu. Rev. Microbiol. **53:**155–187.
51. **Woo, M., R. Hakem, M. S. Soengas, G. S. Duncan, A. Shahinian, D. Kagi, A. Hakem, M. McCurrach, W. Khoo, S. A. Kaufman, G. Senaldi, T. Howard, S. W. Lowe, and T. W. Mak.** 1998. Essential contribution of caspase 3/CPP32 to apoptosis and its associated nuclear changes. Genes Dev. **12:**806–819.
52. **Zimmermann, K. C., C. Bonzon, and D. R. Green.** 2001. The machinery of programmed cell death. Pharmacol. Ther. **92:**57–70.
53. **Zychlinsky, A.** 1993. Programmed cell death in infectious diseases. Trends Microbiol. **1:**114–117.

Editor: J. T. Barbieri